Carbohydrate Polymers 87 (2012) 1131–1138

Contents lists available at SciVerse ScienceDirect

Carbohydrate Polymers

journal homepage: www.elsevier.com/locate/carbpol

Chlorine-free extraction of cellulose from rice husk and whisker isolation

Simone M.L. Rosa, Noor Rehman, Maria Inez G. de Miranda, Sônia M.B. Nachtigall, Clara I.D. Bica*

Chemistry Institute, Federal University of Rio Grande do Sul, PO Box 15003, ZIP 91501-970, Porto Alegre, RS, Brazil

ARTICLE INFO

Article history:
Received 13 May 2011
Received in revised form 1 August 2011
Accepted 24 August 2011
Available online 31 August 2011

Keywords:
Cellulose whiskers
Rice husk
Biomaterials
Microscopy
Peroxide bleaching
Thermal analysis

ABSTRACT

This work reports the isolation of cellulose whiskers from rice husk (RH) by means of an environmental friendly process for cellulose extraction and bleaching. The multistep process begins with the removal of pectin, cutin, waxes and other extractives from rice husk, then an alkaline treatment for the removal of hemicelluloses and lignin, and a two-step bleaching with hydrogen peroxide/tetraacetylethylenediamine (TAED), followed by a mixture of acetic and nitric acids, for further delignification of the cellulose pulp. The techniques of infrared absorption spectroscopy (ATR-FTIR), scanning electron microscopy (SEM), thermogravimetric analysis (TGA), modulated differential scanning calorimetry (MDSC) and X-ray diffraction (XRD) showed that the overall process is adequate to obtain cellulose with high purity and crystallinity. This cellulose was submitted to sulfuric acid hydrolysis with the aim to isolate the whiskers. They showed the typical elongated rod-like aspect as revealed by transmission electron microscopy (TEM) and atomic force microscopy (AFM).

1. Introduction

Rice husk (RH) is one of the major agricultural residues generated as a byproduct during the rice milling process. The Food and Agriculture Organization of the United Nations (FAO) forecasts that the global rice production stands at around 466 million tonnes in 2010/2011 (FAO, 2010). About 23% of this amount consists of RH (Chandrasekhar, Satyanarayana, Pramada, Raghavan, & Gupta, 2003). The Brazilian rice production has been in the order of 12 million tonne/year and Rio Grande do Sul (the southernmost state of Brazil) is responsible for 60% of this production (IBGE, 2010). Most of the RH produced is either used as a bedding material for animals and discarded in land fillings or simply burned in the fields leading to air and soil pollution. The expressive content of about 20% silica in RH and, after burning, more than 90% silica in RH ash have stimulated extensive research which suggested the potential use of RH and its ash as sources of inorganic chemicals (Chandrasekhar et al., 2003). In the present work we propose the use of RH as a new source for obtaining cellulose whiskers and we employ a totally chlorine-free technique (TCF) to extract and bleach cellulose from RH. The isolation of highly pure cellulose from wheat straw (Sun, Sun, Su, & Sun, 2004) and barley straw (Sun, Xu, Sun, Xiao, & Sun, 2005) using totally chlorine-free technologies has been addressed in the scientific literature but not yet from rice husk.

It is well known that the main components of plant fibers are cellulose, hemicelluloses and lignin. Cellulose, which awards the mechanical properties of these materials, is ordered in microfibrils enclosed by the other two components, hemicellulose and lignin (Morán, Alvarez, Cyras, & Vazquez, 2008). Cellulose is the most ubiquitous and abundant natural polymer on the planet, given its presence in plants and its widespread use for ropes, sails, paper, timber for housing and many other applications. By far, the most commercially exploited natural resource containing cellulose is wood (Eichhorn et al., 2010) but cellulose is the main component of several other well employed natural fibers such as cotton, flax, hemp, jute and sisal (Morán et al., 2008). It is expected that the supply of wood at a reasonable price will be insufficient in the future and, apart from the natural fibers mentioned above, agricultural byproducts will become more attractive as sources of cellulose (Leitner, Hinterstoisser, Wastyn, Keckes, & Gindl, 2007).

In recent years there has been a remarkable interest in cellulose fibers of nanometric dimensions. Cellulose whiskers and microfibrils are examples of nanocellulose and result from different isolation methods leading to diverse dimensions and aspect ratios (Siró & Plackett, 2010). Cellulose whiskers are elongated crystalline rod-like nanoparticles being generally isolated by means of acid hydrolysis which removes the amorphous domains existing in cellulose fibers. Cellulose microfibrils in turn are obtained from mechanical treatment being long and flexible nanoparticles which consist of alternating crystalline and amorphous strings (Siqueira, Bras, & Dufresne, 2009). Cellulose whiskers have been isolated from different vegetable sources such as cotton and eucalyptus (Berg, Capadona, & Weder, 2007; Dong, Revol, & Gray, 1998; Hafraoui et al., 2008) and from animal sources such as tunicates (Berg et al., 2007; Hafraoui et al., 2008). Considering vegetable origin, there

* Corresponding author. Tel.: +55 51 3308 7236; fax: +55 51 3308 7304.
E-mail address: claraism@iq.ufrgs.br (C.I.D. Bica).

0144-8617 © 2011 Elsevier Ltd. Open access under the Elsevier OA license.
doi:10.1016/j.carbpol.2011.08.084

are only a few papers which describe the isolation of whiskers from agricultural byproducts, as for example wheat straw (Herbert, Cavaillé, & Dufresne, 1996), pea hull fiber (Chen, Liu, Chang, Cao, & Anderson, 2009), branch-barks of mulberry (Li et al., 2009) and coconut husks (Rosa et al., 2010).

As far as we know, the isolation of cellulose whiskers from rice husk sources has not been yet described in the literature but only the isolation of silicon carbide whiskers from RH (Sujiroti & Leangsuwan, 2003) and of cellulose whiskers from rice straws (Orts et al., 2005). So, the fractionation of lignocellulosic materials of rice husks into its constitutive components by environmental friendly techniques has been the subject of our work with the objective of cellulose whisker isolation. RH and intermediate RH products of the multistep extraction procedure were characterized through scanning electron microscopy (SEM), thermogravimetry (TGA) and attenuated total reflectance-infrared absorption spectroscopy (ATR-FTIR). The purified cellulose was characterized by modulated differential scanning calorimetry (MDSC), wide-angle X-ray diffraction (WAXD) as well as TGA and ATR-FTIR. The whiskers were characterized by transmission electron microscopy (TEM) and atomic force microscopy (AFM). The properties of purified cellulose isolated from rice husk were compared to the properties of commercial microcrystalline cellulose (MCC).

2. Experimental

2.1. Materials

Rice husk was supplied by Engenho Meirebe (Eldorado do Sul/RS, Brazil). Hexane (Fmaia, Brazil), ethanol (Fmaia, Brazil), sodium hydroxide (Labsynth, Brazil), hydrogen peroxide (CAQ Química, Brazil), nitric acid (Fmaia, Brazil), acetic acid (CAQ Química, Brazil), tetra-acetylethylenediamine (TAED) (Acros Organics, New Jersey, USA) were used as received. All solvents and reagents were of analytical grade. Microcrystalline cellulose (MCC) was supplied by Quimsul.

2.2. Procedures

2.2.1. Isolation of cellulose

Rice husks were previously ground. The dried RH was sequentially dewaxed with hexane/ethanol/water in a Soxhlet apparatus. The extractive content was found to be 6.8%. Delignification was done at 121 °C, in autoclave (Stermax 20EHD), using a 5% aqueous NaOH with a 1:30 straw to liquor ratio (g/mL) for 30 min being this step based on a procedure described by Uesu, Pineda, and Hechenleitner (2000), adapted to rice husk. The dispersions were treated with ultrasound for 30 min. In order to remove the remaining hemicelluloses and lignin, the resulting pulp was bleached following a procedure described by Sun, Sun, Su, et al. (2004): the pulp was treated with 2% H_2O_2 and 0.2% TAED solution, at pH 11.8, for 12 h, at 48 °C. The liquor to pulp ratio was 25:1 (mL/g). To purify the cellulose pulp, 5.0 mL of 80% (v/v) acetic acid and 0.5 mL of concentrated nitric acid (70%, v/v) were added to 150 mg of pulp, the mixture was then placed into a preheated oil bath at 120 °C, for 15 min or 30 min. Once cooled, the supernatant was then carefully decanted and the cellulose was washed sequentially with 95% ethanol (20 mL), distilled water (20 mL), and again 95% ethanol (20 mL) to remove extraction breakdown products and traces of nitric acid. Finally, the purified cellulose was dried in an oven at 60 °C until constant mass. Departing from raw rice husks (~9 wt% water), the total yield of extracted cellulose was 28 wt%.

2.2.2. Isolation of the cellulose whiskers

The purified cellulose was mixed with sulfuric acid 64% (w/w) at a ratio of 1:8.75 (g/mL) as described by Dong et al. (1998), at temperature of 25 °C. The hydrolysis time was fixed at 60 min. The reactions were stopped by pouring the mixture into a large amount of cold water. The excess of sulfuric acid was removed by centrifugation (3000 rpm, 30 min), using an ALC centrifuge PK 120, followed by a prolonged dialysis (regenerated cellulose membrane Fisher, cut-off 10,000–14,000 Da) against pure water. This procedure ensured that all ionic materials were removed except the H_3O^+ counterions associated with the sulfate groups on the surface of the whiskers (Dong et al., 1998). The whiskers were further dispersed by an ultrasonic treatment (Ultrasonic equipment Thornton, Model USC-1400).

Although the strong nitric and sulfuric acids were used in the overall procedure, the effluents turned to be dilute and were easily neutralized.

2.3. Characterization

2.3.1. Rice husk and cellulose

Scanning electron micrographs of dried RH, extractive free and alkaline treated RH were obtained using a JEOL® microscope JSM 6060 operating at 20 kV. The test specimens were attached to an aluminum stub and sputtered with gold to eliminate the electron charging effects.

WAXD experiments were performed using a Siemens D-500 diffractometer. Purified RH cellulose (after 30 min bleaching and also called as RH cellulose) and MCC were scanned in the reflection mode using an incident X-ray of CuKα with wavelength of 1.54 Å at a step width of 0.05° min^{-1} from $2\theta = 0$ to 40°. The Segal method was used to calculate the crystallinity of the samples (Thygesen, Oddershede, Lilholt, Thomsen, & Stahl, 2005). Eq. (1) was used to calculate the sample crystallinity (X_{CR}).

$$X_{CR} = \frac{I_{200} - I_{AM}}{I_{200}} \times 100\% \quad (1)$$

where I_{200} is the height of the 200 peak, which represents both crystalline and amorphous material and I_{AM} is the lowest height between the 200 and 110 peaks, which represents amorphous material only.

In our study we performed a preliminary experiment in a muffle furnace under air atmosphere to determine the ash content of rice husk.

TGA scans were carried out from 35 to 700 °C at a heating rate of 10 °C min^{-1} and under inert atmosphere of N_2 in a flux of 50 mL min^{-1} (TA Instruments model TGA Q5000 IR). Sample weight was typically kept at 17 mg. The TGA microbalance has a precision of ±0.1 μg.

MDSC was performed using a DSC Q2000 differential scanning calorimeter from TA Instruments. Sample weight was kept at ~7 mg using hermetically sealed pans with a pinhole in the lid. Two procedures were made using purified RH cellulose (after 30 min bleaching) in MDSC. In the first one, the samples were analysed as obtained after bleaching treatment, equilibrated at 35 °C for 5 min and heated up to 395 °C at heating rate of 5 °C min^{-1}. In addition, a second procedure was made applying a ramp of 30 °C min^{-1} from room temperature to 150 °C and equilibrating at this temperature for 5 min to remove adsorbed water, as suggested in the literature (Cabrales & Abidi, 2010; Picker & Hoag, 2002). After this isothermal condition, samples were cooled until 35 °C and a second scan was performed at 5 °C min^{-1} up to 395 °C. The MDSC analyses were carried on under inert atmosphere of N_2 in a flux of 50 mL min^{-1} using an amplitude of temperature modulation of ±1 °C and a period modulation of 60 s.

Structural changes between MCC, RH, RH intermediate products and purified RH cellulose were revealed by using ATR-FTIR with 64 scans and a resolution of 2 cm^{-1}, in a Nicolet 6700 spectrophotometer.

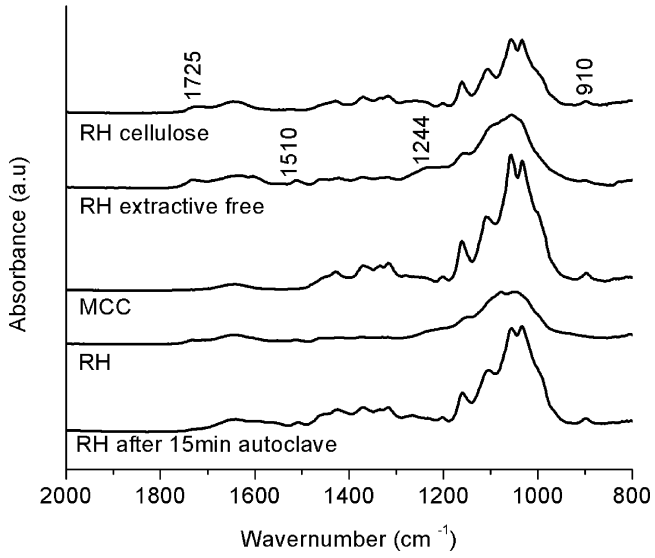

Fig. 1. ATR-FTIR spectra for RH, RH extractive-free, alkaline treated RH (RH after 15 min autoclave), RH cellulose (after 30 min bleaching) and commercial cellulose (MCC) in the range from 2000 to 800 cm^{-1}.

2.3.2. Cellulose whiskers

For the TEM images, drops of RH whisker aqueous suspensions were deposited on glow-discharged carbon coated TEM grids and the excess of water was let to evaporate. The specimens were negatively stained with 2% uranyl acetate and observed using a JEOL JEM 1200FxII electron microscope operating at 80 kV. The whisker dimensions were determined with the aid of the Image Tools software.

AFM observations were carried out using a Molecular Imaging Pico Plus microscope operating in air and intermittent contact mode with a Micromash NC36 tip. Drops of dilute aqueous suspensions of RH cellulose whiskers were deposited onto freshly cleaved mica. After 30 min, the excess liquid was removed and the remaining film allowed to dry.

3. Results and discussion

3.1. Characterization of the rice husk and rice husk cellulose

3.1.1. Spectroscopic characterization

FTIR spectroscopy has been extensively used in cellulose research, since it presents a relatively easy method of obtaining direct information on chemical changes that occur during various chemical treatments (Sun, Sun, Zhao, & Sun, 2004). By identifying the functional groups present, FTIR allows to know about the chemical structure of each compound. In this work FTIR was employed with the aim of verifying if lignin and hemicelluloses were removed from the extracted cellulose.

In this work FTIR spectra of RH, RH free of extractives, commercial cellulose (MCC), and purified RH cellulose were obtained. All samples presented two main absorbance regions. The first one at high wavenumbers corresponds to the range 2700–3500 cm^{-1} (Fig. 1S, Supplementary material), and the second one at lower wavenumbers, to the range 800–1800 cm^{-1} approximately. The latter can be seen in Fig. 1. The broad absorption band with peaks, depending on the sample, located from 3330 to 3360 cm^{-1} is due to stretching of –OH groups and that one near 2900 cm^{-1} is related to the C–H stretching vibrations.

The band at 1640 cm^{-1} could be assigned to the C=C stretching of aromatic rings of lignin but it is also present in the spectrum of commercial cellulose. According to various authors (Morán et al., 2008; Sun, Sun, Su, et al., 2004; Zuluaga, Putaux, Restrepo, Mondragon, & Gañán, 2007), this band relates to the bending mode of adsorbed water. All samples were carefully dried before the ATR-FTIR spectra were taken, but, as reported in the literature, it is difficult to completely dry cellulose due to its strong interaction with water (Morán et al., 2008; Szczesniak, Rachocki, & Tritt-Goc, 2008). All materials analysed presented this absorption band but specific absorptions can also be seen in the spectra. The absorption band at 1176 cm^{-1} corresponds to C–O–C asymmetrical bridge stretching. As pointed out by Sun, Sun, Su, et al. (2004), a strong peak at 1049 cm^{-1} arises from C–O–C pyranose ring skeletal vibration. In Fig. 1 it can be seen that this peak changes its form in the RH cellulose as far as it appears as a doublet. In comparison to the spectrum of commercial cellulose, it can be concluded that hemicelluloses were extensively removed. The sharp peak at 910 cm^{-1} is characteristic of β-glycosidic linkages between the sugar units (Sun, Sun, Su, et al., 2004). The spectra of RH and RH free of extractives show two absorptions characteristic of lignin: a weak band at 1510 cm^{-1} (also C=C stretching of aromatic ring) and a broad shoulder at 1244 cm^{-1} (C–O stretching of the ether linkage) which are absent in the spectrum of RH cellulose as well as that of commercial cellulose. According to Viera et al. (2007), the absence of these bands indicates that most of the lignin was removed. So in RH cellulose the extraction procedures removed most of lignin polymers because of the disappearance of the lignin-associated absorbances at 1510 cm^{-1} and 1244 cm^{-1}. In the spectrum of RH cellulose it can also be identified a peak at 1725 cm^{-1} (C=O of ketone) which probably arises from partial acetylation of RH cellulose during the second bleaching step where acetic acid is employed as also mentioned by other authors (Morán et al., 2008; Sun, Sun, Su, et al., 2004; Zuluaga et al., 2007). In the spectra of RH and RH free of extractives a peak at 1734 cm^{-1} can be seen which can also be assigned to C=O of ketone but due to hemicelluloses. Fig. 1 also shows an ATR-FTIR spectrum of extractive-free cellulose pulp obtained after 15 min of alkaline treatment, in autoclave, and before the bleaching steps. In this spectrum there is not any absorbance in the carbonyl region.

3.1.2. Scanning electron microscopy (SEM)

By SEM it was possible to detect different effects on the RH surface according to the stages of pre-extraction and pulping, as shown in Fig. 2. The changes in the outer epidermis show the chemical attack suffered by the material at different stages.

In comparison to extractive-free rice husk (Fig. 2a), after 15 min of alkaline treatment in autoclave, it can be seen that the rice husk particles changed from flat to rolled shape (Fig. 2b). Fig. 2c shows the surface of extractive-free rice husk with the presence of silica particles. A similar aspect of RH surface was also reported by Chandrasekhar et al. (2003). Fig. 2d shows that these particles were removed after 15 min in autoclave. In Fig. 2e filaments can be seen on the outer epidermis in the regions where protuberances were removed after 30 min in autoclave. Fig. 2f shows that after 1 h in autoclave the surface did not change significantly. So 30 min in autoclave was chosen as the optimum time. By comparing Fig. 2g (15 min in autoclave) and Fig. 2h (30 min in autoclave) it can be noticed that the inner epidermis is also modified when the autoclave treatment is increased to 30 min. This alkaline treatment in autoclave also causes a reduction of the average size of RH particles (Fig. 2S, Supplementary material).

3.1.3. Thermogravimetric analysis (TGA)

Fig. 3 shows the thermal degradation pattern of the commercial cellulose (MCC), crude RH, and RH cellulose (after 15 min and 30 min bleaching). All samples showed a thermal event below 150 °C corresponding to dehydration. The mass loss of water in this step was determined from 45 °C to 150 °C. It was about 3.8 wt% for

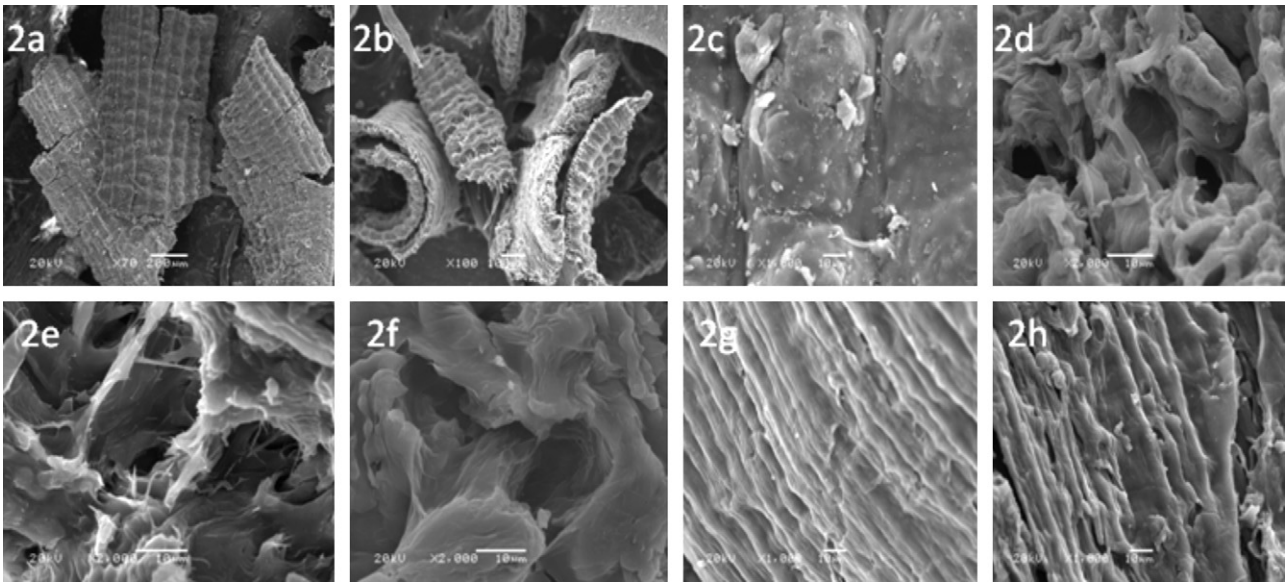

Fig. 2. SEM micrographs of RH after various stages of chemical attack: a, b) outer epidermis of RH extractive-free (bars: 200 μm and 10 μm, respectively); c, d) RH outer epidermis after 15 min in autoclave (100 μm and 10 μm, respectively); e) RH outer epidermis after 30 min in autoclave (bar: 10 μm, both); f) RH outer epidermis after 60 min in autoclave (bar: 10 μm); g) RH inner epidermis after 15 min in autoclave (bar: 10 μm); h) RH inner epidermis after 30 min in autoclave (bar: 10 μm).

MCC, 9.0 wt% for crude RH, 5.8 wt% for RH cellulose after 15 min bleaching and 5.7 wt% for RH cellulose after 30 min bleaching. The effective thermal degradation of the RH constituents begins above 200 °C and refers to bond cleavage of hemicellulose, cellulose and lignin.

It is possible to verify that RH cellulose showed higher thermal stability than the precursor RH, since in these samples the components that start to degrade at lower temperature had been removed. The crude RH main decomposition peak is considerably wider than those of the other samples due to the decomposition of hemicelluloses and lignin. Commercial cellulose and RH cellulose decomposed in a single step. This behavior suggests the absence of hemicellulose and lignin in the RH cellulose obtained. The DTG curve of RH cellulose does not show the shoulder close to the cellulose peak that refers to the hemicellulose. This is in accordance with the FTIR results previously shown. The maximum rate of decomposition of RH cellulose occurred at 345 °C. This temperature agrees well with the value of 348 °C found by Morán et al. (2008) for the decomposition peak of commercial cellulose and 355 °C found by Yang, Yan, Chen, Lee, & Zheng (2007), determined at same heating rate. The commercial cellulose showed higher T_{max} than the RH cellulose isolated in this step. According to the literature, the higher the decomposition temperature obtained by thermogravimetric analysis the greater the crystallinity of cellulose (Alemdar & Sain, 2008; Chen et al., 2011; Uesu, Pineda, & Hechenleitner, 2000). However, the discussions have been recently improved considering other effects that can influence the temperature peak of degradation: presence of substances bonded to microfibril surfaces (Vila, Barneto, Fillat, Vidal, & Ariza, 2011), crystal size of cellulose (Kim, Eom, & Wada, 2010) and the atmosphere environment used (usually nitrogen or air) (Mamleev, Bourbigot, & Yvon, 2007; Vila et al., 2011).

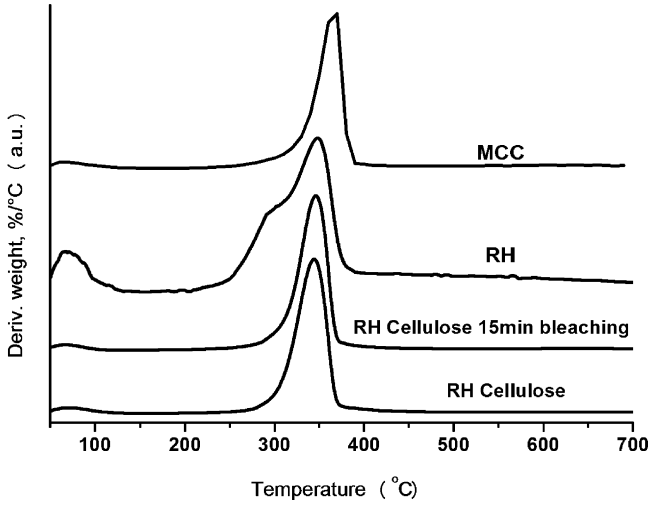

Fig. 3. DTGA curves for commercial cellulose (MCC), RH, RH cellulose after 15 min bleaching and RH cellulose (30 min bleaching).

RH presented a high residual mass at the end of the experiment (700 °C), around 26%. The ash content of rice husk determined under air atmosphere in this work was 16 wt% at 1000 °C. The result agrees perfectly well with Zhao et al. (2009). Even considering that the analysis was performed under nitrogen atmosphere, this was an especially high value and it was related to the high silica content of RH (Rosa, Nachtigall, & Ferreira, 2009). At 700 °C residues of about 8% for commercial cellulose, 15% for RH cellulose after 15 min bleaching and 11% for RH cellulose after 30 min bleaching can be determined from the TGA curves (Fig. 3S, Supplementary material). As indeed evidenced by the X-ray diffraction study, the crystallinity index of RH cellulose is lower than that of the commercial cellulose. Another explanation may be related to the partial acetylation of RH cellulose evidenced by the presence of an absorption at 1725 cm^{-1} in the ATR-FTIR spectrum.

3.1.4. Modulated differential scanning calorimetry (MDSC)

Modulated differential scanning calorimetry (MDSC) permits the separation of the total heat flow signal into its reverse heat flow and non-reverse heat flow components. The separation is based not only on thermodynamic reversibility but also on changes occurring when a sinusoidal modulation is overlaid on a conventional linear heating rate during an experiment. In this sense, MDSC arises as an exciting way to increase the understanding of rice husk cellulose thermal properties. The effects of temperature on amorphous and crystalline regions of rice husk cellulose were studied by MDSC.

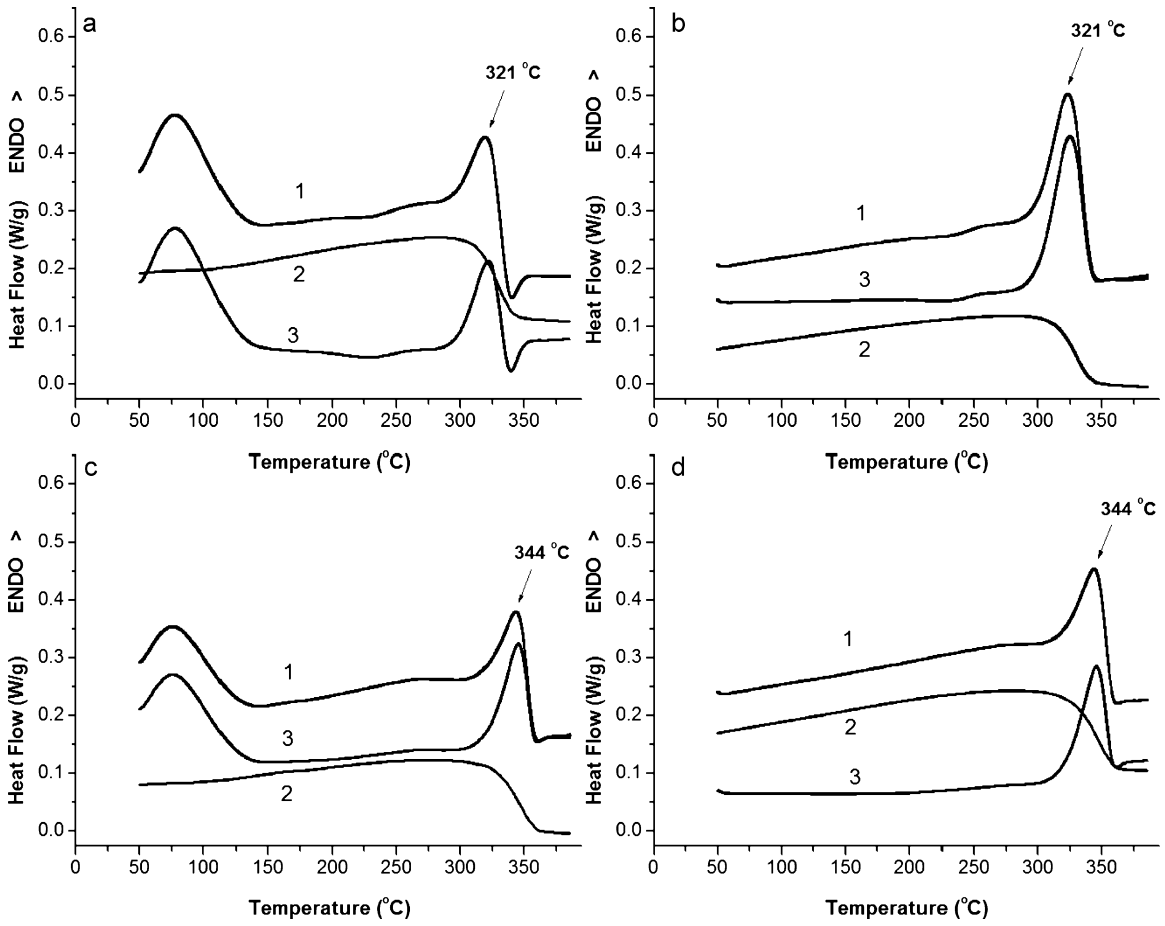

Fig. 4. MDSC curves of total (1), reverse (2) and non-reverse (3) heat flow at 5 °C min^{-1}: (a) RH cellulose (30 min bleaching), under first procedure; (b) RH cellulose (30 min bleaching), under second procedure; (c) MCC, under first procedure; (d) MCC, under second procedure.

Considering literature using DSC technique, as reported by Morán et al. (2008) and Yang et al. (2007), the fusion of the crystalline fraction of some types of cellulose shows a narrow endothermic peak close to 330 °C. This transition can move to lower temperatures depending on factors such as molecular weight, amount of amorphous content, crystallite sizes, etc. Sometimes, an exothermic peak is found in the same region, which has been related to a degradation process (Morán et al., 2008). According to Mamleev et al.'s studies (2007), a depolymerization by transglycosylation occurs at 310 °C during cellulose pyrolysis. As both events can be superimposed, they cannot be easily distinguished in many cases.

Fig. 4a shows the heat flow curves of RH cellulose analysed by MDSC. Considering total and non-reverse heat flow curves, they show two main events. The first endothermic peak observed below 150 °C is due to loss of water. The second endothermic transition starts around 270 °C with a peak at 320 °C and is related to cellulose melting. A smooth exothermic transition can be detected near 340 °C. This event has its onset overlapped with the end of the endothermic region and can be related to the depolymerization of cellulose as supported by the equivalent peak in the non-reverse heating curve. Such conclusion is also corroborated by the TGA study which shows a maximum of weight loss for RH cellulose in the same temperature region. On the other hand, an important change in the heat capacity of the medium can also be seen between 300 °C and 330 °C in the reverse heat flow curve. This indicates a change in chemical composition as a result of the depolymerization reaction. The absence of an endotherm in reversing signal indicates that this thermal event is a kinetic transformation. By visual inspection of the pan, very few solid residues were found at this stage and charring process was evident.

Fig. 4b shows the MDSC curves of RH cellulose submitted to the second procedure described in the experimental section, with an isothermal step to eliminate water. As expected, it was not found any peak due to water release. A well-defined endothermic transition is present beyond 300 °C which is similar to that of Fig. 4a being related to melting and volatilization as well. However the small exothermic peak following this transition was not clearly seen in the total and non-reverse curves. The thermograms profiles of RH cellulose are very similar to those of MCC which are shown in Fig. 4c and d. In comparison to MCC, the peak maximum of the endothermic transition detected beyond 300 °C occurred at lower temperature for RH cellulose (as assigned by arrows T_{RH} = 321 °C, in Fig. 4a and b, and T_{MCC} = 344 °C in Fig. 4c and d) independently of water presence as it was observed in total and non-reverse heating curves.

In this study, it was observed that all samples showed well-defined endothermic peaks corresponding to the fusion of its crystalline part, as shown in Fig. 4a–d. However, cellulose samples with water adsorbed (Fig. 4a and c) showed more clearly the exothermic peaks following melting. This suggests that the degradation mechanism responsible for the exothermic peak is affected by the presence of water.

3.1.5. Wide angle X-ray diffraction (WAXD)

It can be observed in Fig. 5 that the major crystalline peak for each sample occurred at around $2\theta = 22°$ which represents the cellulose crystallographic plane (2 0 0). The crystallinity index of

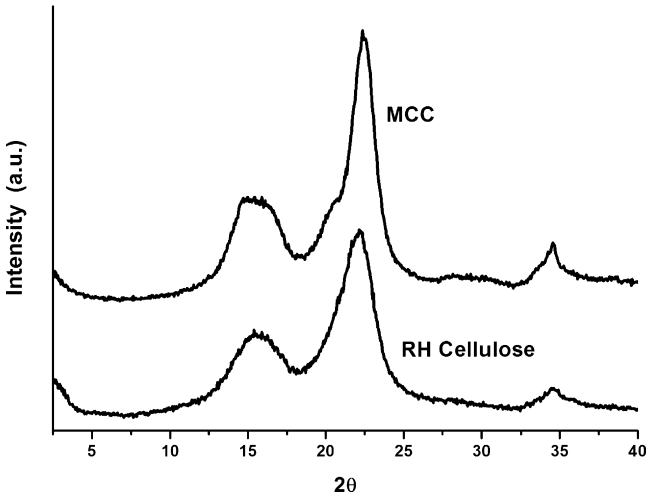

Fig. 5. X-ray diffraction patterns of MCC and RH cellulose (30 min bleaching).

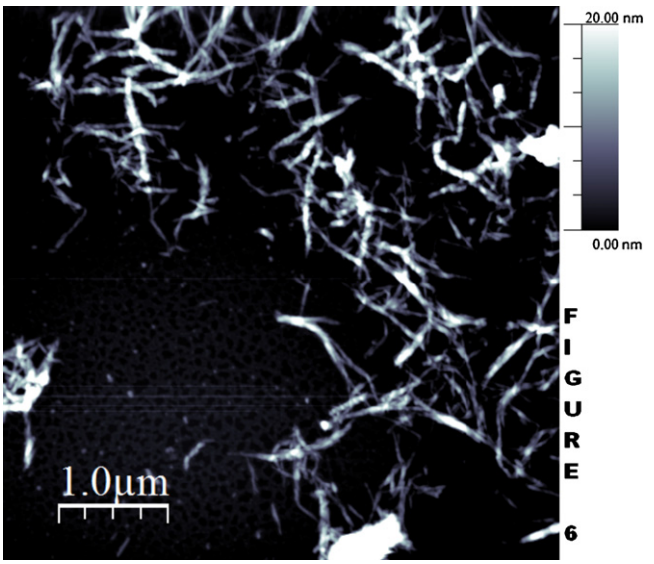

Fig. 6. AFM image of RH cellulose whiskers obtained after 60 min of acid hydrolysis.

RH cellulose (calculated by Segal formula) was approximately 67% while that of MCC was estimated as 79%. For comparison, the crystallinity index of other samples, as reported in the literature, was found to be around 66% for potato tuber cellulose, 68% for rice straw cellulose and 71% for wood cellulose (Abe & Yano, 2009). It can be concluded that the procedure employed in this study for cellulose extraction from rice husk is adequate for obtaining samples with high crystallinity. It was reported that highly crystalline fibers and fibril aggregates could be more effective in achieving higher reinforcement for composite materials (Cheng, Wang, Rials, & Lee, 2007). In addition it can be noticed in Fig. 5 that RH cellulose can be classified as cellulose I, since there is no doublet in the intensity of the peak at ca. $2\theta = 22^{\circ}$. A similar finding was reported by Morán et al. (2008) for sisal cellulose extracted by other procedures.

3.2. Characterization of cellulose whiskers

Basically, microscopy has been the preferred technique for the morphological characterization in studies involving cellulose whiskers. In this study, AFM and TEM were used to investigate the morphology and size of the dispersed structures.

The atomic force micrograph in Fig. 6 shows the sample obtained after 60 min of hydrolysis. It was possible to see the isolated cellulose fibrils free from the other components of rice husks. Most of the hydrogen bonds that kept the whiskers associated were probably disrupted after this procedure. However, some aggregates are still present.

By TEM (Fig. 7a and b), structures in the form of needles ranging from 100 to 400 nm in length and 6 to 14 nm in width were observed. The average length value was $L = (143 \pm 64)$nm while the average thickness was $d = (8 \pm 2)$nm. Such dimensions are comparable to those of whiskers originating from cotton (Beck-Candanedo, Roman, & Gray, 2005; Bica, Borsali, Rochas, & Geissler, 2006; Hafraoui et al., 2008), wood (Beck-Candanedo et al., 2005), pea hull fiber (Chen et al., 2009) and coconut husks (Rosa et al., 2010). The RH whiskers show lengths shorter than in the case of branch-barks of mulberry (Li et al., 2009) but RH whiskers are much thinner. The aspect ratio shows an average value near 18. In Fig. 6 some RH whiskers appeared more aggregated in the form of bundles as also observed by Heux, Chauve, and Bonini (2000) in the case of cotton whiskers. According to Hafraoui et al. (2008), such nanostructures can be composed of a varying number of parallel subunits of cellulose chains. The high aspect ratio of the cellulose whiskers obtained from rice husk indicates that these structures exhibit promising

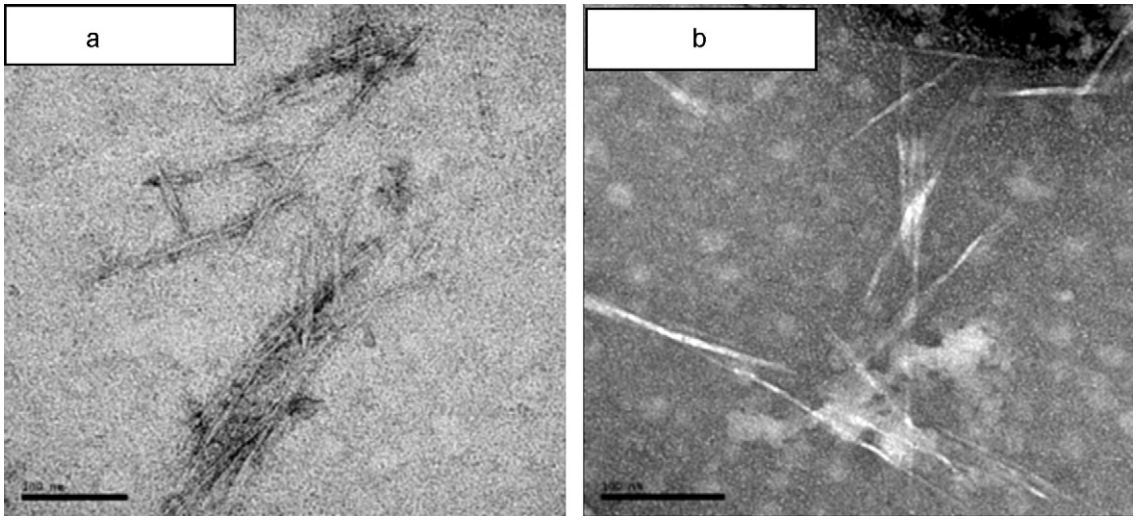

Fig. 7. TEM images of RH cellulose whiskers (bars correspond to 100 nm).

behavior as nanofillers for polymer matrices, providing valorization of this worldwide produced agricultural waste.

4. Conclusions

Residues from plants are interesting alternatives as cellulose sources for several applications. In this work a chlorine-free procedure for the isolation of cellulose from rice husk was shown to be very efficient. The overall process does not produce any toxic effluents. On the basis of the whole cellulose content expected for rice husk, this method resulted in a yield around 74%. TGA analysis performed under nitrogen showed high residual mass for RH at 700 °C. This can be partially attributed to the high silica content of the material. In our study, the ash content of RH at 1000 °C was determined to be 16 wt%. FTIR, TGA and MDSC analyses agreed well with respect to the elimination of hemicellulose and lignin from rice husk after the purification procedure used to isolate cellulose. WAXD experiments indicated that the crystallinity of RH cellulose (67%) was lower than that of MCC (79%). Lower crystallinity has been pointed out as a factor, among others, that can lower the thermal degradation temperature. The decomposition temperature of RH cellulose was found to be lower than commercial microcrystalline cellulose. Besides water elimination, the MDSC analyses showed one main endothermic event for cellulose samples (RH cellulose and MCC), which was related to the melting of cellulose crystals. The TGA and MDSC results agree well with respect to the thermal stability of rice husk cellulose and helped to improve the knowledge on the complex behavior of cellulose degradation.

Cellulose whiskers were successfully obtained by sulfuric acid hydrolysis of the rice husk cellulose. According to TEM and AFM images, it was possible to isolate needle-like structures of cellulose whiskers, with sizes varying from 6 to 14 nm in width and 100–400 nm in length. The average values of length and thickness of these whiskers give an aspect ratio around 18. Such a value of aspect ratio is adequate for application of RH whiskers as nanofillers in polymer matrices. In this way the use of rice husk as a novel material source allows to obtain new particles with nanometric dimensions widening the supply of nanostructured materials usable for polymer nanocomposites.

Acknowledgements

The authors would like to thank Conselho Nacional de Desenvolvimento Científico e Tecnológico (CNPq) for grant 474278/2007-7 and fellowship TWAS/CNPq; Coordenação de Aperfeiçoamento de Pessoal de Ensino Superior (CAPES) and Fundação de Amparo à Pesquisa do Estado do Rio Grande do Sul (FAPERGS) for fellowships (also CAPES/REUNI); Centro de Microscopia Eletrônica of the Federal University of Rio Grande do Sul (CME/UFRGS) and Ms. M. Queiroz for technical assistance during the TEM and SEM analyses; Mr. O. Machado (Instituto de Física/UFRGS) for performing the WAXD measurements, Dr. J. Vaghetti (IQ/UFRGS) for technical assistance during TGA and MDSC analyses and Ms. N. Reis for help in the first experiments of this project.

Appendix A. Supplementary data

Supplementary data associated with this article can be found, in the online version, at doi:10.1016/j.carbpol.2011.08.084

References

Abe, K., & Yano, H. (2009). Comparison of the characteristics of cellulose microfibril aggregates of wood, rice straw and potato tuber. *Cellulose*, *16*, 1017–1023.

Alemdar, A., & Sain, M. (2008). Isolation and characterization of nanofibers from agricultural residues – Wheat straw and soy hulls. References and further reading may be available for this article. To view references and further reading you must purchase this article. *Bioresource Technology*, *99*, 6554–6561.

Beck-Candanedo, S., Roman, M., & Gray, D. G. (2005). Effect of reaction conditions on the properties and behavior of wood cellulose nanocrystal suspensions. *Biomacromolecules*, *6*, 1048–1054.

Berg, O., Capadona, J. R., & Weder, C. (2007). Preparation of homogeneous dispersions of tunicate cellulose whiskers in organic solvents. *Biomacromolecules*, *8*, 1353–1357.

Bica, C. I. D., Borsali, R., Rochas, C., & Geissler, E. (2006). Dynamics of cellulose whiskers spatially trapped in agarose hydrogels. *Macromolecules*, *39*, 3622–3627.

Cabrales, L., & Abidi, N. (2010). On the thermal degradation of cellulose in cotton fibers. *Journal of Thermal Analysis & Calorimetry*, *102*, 485–491.

Chandrasekhar, S., Satyanarayana, K. G., Pramada, P. N., Raghavan, P., & Gupta, T. N. (2003). Processing, properties and applications of reactive silica from rice husk – An overview. *Journal of Materials Science*, *38*, 3159–3168.

Chen, Y., Liu, C., Chang, P. R., Cao, X., & Anderson, D. P. (2009). Bionanocomposites based on pea starch and cellulose nanowhiskers hydrolysed from pea hull fibre: Effect of hydrolysis time. *Carbohydrate Polymers*, *76*, 607–615.

Chen, W., Yu, H., Liu, Y., Chen, P., Zhang, M., & Hai, Y. (2011). Individualization of cellulose nanofibers from wood using high-intensity ultrasonic combined with chemical pretreatments. *Carbohydrate Polymers*, *83*, 1804–1811.

Cheng, Q., Wang, S., Rials, T. G., & Lee, S.-H. (2007). Physical and mechanical properties of polyvinyl alcohol and polypropylene composite materials reinforced with fibril aggregates isolated from regenerated cellulose fibers. *Cellulose*, *14*, 593–602.

Dong, X. M., Revol, J.-F., & Gray, D. G. (1998). Effect of microcrystallite preparation conditions on the formation of colloid crystals of cellulose. *Cellulose*, *5*, 19–32.

Eichhorn, S. J., Dufresne, E. A., Araguren, E. M., Marcovich, E. N. E., Capadona, E. J. R., Rowan, E. S. J., et al. (2010). Review: Current international research into cellulose nanofibres and nanocomposites. *Journal of Materials Science*, *45*, 1–33.

FAO (2010). Global cereal supply and demand brief. Crop prospects & food situation (no. 4 (Dec), p. 5). http://www.fao.org/giews/ Accessed 06.02.11.

Hafraoui, S., Nishiyama, Y., Putaux, J.-L., Heux, L., Dubreuil, F., & Rochas, C. (2008). The shape and size distribution of crystalline nanoparticles prepared by acid hydrolysis of native cellulose. *Biomacromolecules*, *9*, 57–65.

Herbert, W., Cavaillé, J. Y., & Dufresne, A. (1996). Thermoplastic nanocomposites filled with wheat straw cellulose whiskers. Part I: Processing and mechanical behavior. *Polymer Composites*, *17*, 604–611.

Heux, L., Chauve, G., & Bonini, C. (2000). Nonflocculating and chiral-nematic self-ordering of cellulose microcrystals suspensions in nonpolar solvents. *Langmuir*, *16*, 8210–8212.

IBGE (2010). Grupo de Coordenação de Estatísticas Agropecuárias (Dec 2010). http://www.ibge.gov.br/home/estatistica/indicadores/agropecuaria/lspa/lspa_201012_12.shtm Accessed 06.02.11.

Kim, U., Eom, S. H., & Wada, M. (2010). Thermal decomposition of native cellulose: Influence on crystalline size. *Polymer Degradation and Stability*, *95*, 778–781.

Leitner, J., Hinterstoisser, B., Wastyn, M., Keckes, J., & Gindl, W. (2007). Sugar beet cellulose nanofibril-reinforced composites. *Cellulose*, *14*, 419–425.

Li, R., Fei, J., Cai, Y., Li, Y., Feng, J., & Yao, J. (2009). Cellulose whiskers extracted from mulberry – A novel biomass production. *Carbohydrate Polymers*, *76*, 94–99.

Mamleev, V., Bourbigot, S., & Yvon, J. (2007). Kinetic analysis of the thermal decomposition of cellulose: The main step of mass loss. *Journal of Analytical and Applied Pyrolysis*, *88*, 151–165.

Morán, J. I., Alvarez, V. A., Cyras, V. P., & Vazquez, A. (2008). Extraction of cellulose and preparation of nanocellulose from sisal fibers. *Cellulose*, *15*, 149–159.

Orts, W. J., Shey, J., Imam, S. H., Glenn, G. M., Guttman, M. E., & Revol, J. F. (2005). Application of cellulose microfibrils in polymer nanocomposites. *Journal of Polymers and the Environment*, *13*, 301–306.

Picker, K. M., & Hoag, S. W. (2002). Characterization of the thermal properties of microcrystalline cellulose by modulated temperature differential scanning calorimetry. *Journal of Pharmaceutical Sciences*, *91*, 342–349.

Rosa, S. M. L., Nachtigall, S. M. B., & Ferreira, C. A. (2009). Thermal and dynamic-mechanical characterization of rice-husk filled polypropylene composites. *Macromolecular Research*, *17*(1), 8–13.

Rosa, M. F., Medeiros, E. F., Malmonge, J. A., Gregorsky, K. S., Wood, D. F., Mattoso, L. H. C., et al. (2010). Cellulose nanowhiskers from coconut husk fibers: Effect of preparation conditions on their thermal and morphological behavior. *Carbohydrate Polymers*, *81*(*1*), 83–92.

Siqueira, G., Bras, J., & Dufresne, A. (2009). Cellulose whiskers versus microfibrils: Influence of the nature of the nanoparticle and its surface functionalization on the thermal and mechanical properties of nanocomposites. *Biomacromolecules*, *10*, 425–432.

Siró, I., & Plackett, D. (2010). Microfibrillated cellulose and new nanocomposite materials: A review. *Cellulose*, *17*, 459–494.

Sujiroti, K., & Leangsuwan, P. (2003). Silicon carbide formation from pretreated rice husks. *Journal of Materials Science*, *38*, 4739–4744.

Sun, X. F., Sun, R. C., Su, Y., & Sun, J. X. (2004). Comparative study of crude and purified cellulose from wheat straw. *Journal of Agricultural Food Chemistry*, *52*, 839–847.

Sun, J. X., Sun, X. F., Zhao, H., & Sun, R. C. (2004). Isolation and characterization of cellulose from sugarcane bagasse. *Polymer Degradation & Stability*, *84*, 331–339.

Sun, J. X., Xu, F., Sun, X.-F., Xiao, B., & Sun, R. C. (2005). Physico-chemical and thermal characterization of cellulose from barley straw. *Polymer Degradation & Stability*, *88*, 521–531.

Szczesniak, L., Rachocki, A., & Tritt-Goc, J. (2008). Glass transition temperature and thermal decomposition of cellulose powder. *Cellulose*, *15*, 445–451.

Thygesen, A., Oddershede, J., Lilholt, H., Thomsen, A. B., & Stahl, K. (2005). On the determination of crystallinity and cellulose content in plant fibres. *Cellulose*, *12*, 563–576.

Uesu, C. N. Y., Pineda, E. A. G., & Hechenleitner, A. A. W. (2000). Microcrystalline cellulose from soybean husk: Effects of solvent treatments on its properties as acetylsalicylic acid carrier. *International Journal of Pharmaceutics*, *206*, 85–96.

Viera, R. G. P., Rodrigues, G., Assunção, R. M. N., Meireles, C. S., Vieira, J., & Oliveira, G. S. (2007). Synthesis and characterization of methylcellulose from sugarcane bagasse cellulose. *Carbohydrate Polymers*, *67*, 182–189.

Vila, C., Barneto, A. G., Fillat, A., Vidal, T., & Ariza, J. (2011). Use of thermogravimetric analysis to monitor the effect of natural laccase mediators on flax pulp. *Bioresource Technology*, *102*, 6554–6561.

Yang, H., Yan, R., Chen, H., Lee, D. H., & Zheng, C. (2007). Characteristics of hemicellulose, cellulose and lignin pyrolysis. *Fuel*, *86*, 1781–1788.

Zhao, Q., Zhang, B., Quan, H., Yamb, R. C. M., Yuen, R. K. K., & Li, R. K. Y. (2009). Flame retardancy of rice husk-filled high-density polyethylene ecocomposites. *Composites Science and Technology*, *69*, 2675–2681.

Zuluaga, R., Putaux, J.-L., Restrepo, A., Mondragon, I., & Gañán, P. (2007). Cellulose microfibrils from banana farming residues: Isolation and characterization. *Cellulose*, *14*, 585–592.